CO-025

THE CONTRIBUTE OF THERMAL INFORMATION TO MAP VULNERABILITY OF INDUSTRIAL COASTAL AREAS

TARANTINO E., AIELLO A., CAPRIOLI M.
Politecnico di Bari, BARI, ITALY

ABSTRACT

This study explores the potentiality of high resolution thermal infrared (TIR) satellite imagery to map static and dynamic variation of temperature on two high risk coastal areas. Specifically, the analysis focuses on the impacts generated by industrial cooling water injection and the increase in seawater temperature over time on the Apulia coast (Italy). For such purpose single and multiple acquisitions TIR data derived from LANDSAT and ASTER satellite sensors will be used to observe SST (Sea Surface Temperature) in order to provide insight on spatial variability a of temperature, totally lacking of conventional in situ measurements. The synoptic view given by satellite images will be used to produce SST thematic cartography processed in an integrated RS/GIS software environment highlighting critical situations of the high polluted study areas.

KEYWORDS

Thermal Infrared; LANDSAT ETM+; ASTER; Sea Surface Temperature

INTRODUCTION

The concept of environmental quality of coastal and marine systems requires a lot of data and information on a wide range of parameters because of its complexity. In recent years, levels of contaminants have increased as a consequence of human activities, altering sometimes natural hydrodynamics of coastal and marine systems. Of the many environmental parameters identified as priorities for climate change research by the Intergovernmental Panel on Climate Change (IPCC), sea surface temperature (SST) is one of the most important [IPCC, 2010]. Understanding SST changes is critical for global and local change detection studies and contributes to develop emission scenarios and policies by which potential anthropogenic effects on global climate may be mitigated. Unfortunately, monitoring long-term changes in SST is hindered by the size of the world ocean, changes in instrumentation, and the difficulty in taking detailed measurements at sea level.

Satellite technology has improved upon our ability to measure SST by allowing frequent and global coverage. While long-term regional and global satellite SST products do exist, they are often limited in terms of spatial resolution and consistency due to uneven sensor performance. Improved spatial and radiometric resolution, regular sampling, and synoptic perspective of recent aerospace platforms make them well suited to improvement of SST measurement capability [Bondur, 2005].

Thermal infrared (TIR) sensors have been successfully deployed at global scale on operational meteorological satellites for over 30 years to provide images of cloud top and sea surface temperatures (SST). Since TIR radiance depends on both the temperature and emissivity of the target, it is difficult to measure land surface temperatures. For, the emissivity will vary as the land cover changes. On the other hand, over water emissivity is known and nearly constant (98%), approaching the behavior of a perfect blackbody radiator [Klemas, 2009]. Considering that the TIR radiance measured over the oceans will primarily vary with SST, an accurate determination of the SST accurately (± 0.5 ºC) can be performed through some atmospheric corrections [Ikeda and Dobson,1995]. Accurate long-time SST observations are important to a wide range of oceanographic studies and global-scale events, e.g. to investigate western boundary currents, such as the Gulf Stream and Kuroshio, or to monitor El Niño events of major upwelling areas and the elevated SSTs damaging coral reefs which support a large diversity of sea life.

At local scale, TIR data can aid identifying a severe environmental phenomenon: thermal pollution resulting from power plant and industry discharges of water used in cooling processes. Aquatic life gets affected as the seemingly harmless thermal pollution lowers dissolved oxygen and increases respiration rates, killing an ever increasing quantity of fish in their positive feedback cycle. The density and viscosity of water also decrease as temperature increases. This results in a faster settling of suspended solids. The rate of evaporation significantly increases too as temperature increases, resulting in a greater wastage of water in the form of its vapor.

Among various medium resolution satellite sensors, LANDSAT sensor proved to be useful in studying inland water processes [Rogers et al., 1976], in clarity and color of water associated with changes in sediment input or the amount of chlorophyll [Choubey, 1998]. Thermal infrared data were processed to

look at changes in the surface temperature associated with upwellings or changes in circulation [Schladow et al., 2004]. In 1999, a next generation of LANDSAT sensors was launched, including the Enhanced Thematic Mapper Plus (ETM+). ETM+ also has a single thermal band (10.31–12.36 μm), but with an improved spatial resolution of 60 m and improved NEΔT (*noise-equivalent temperature difference*) of 0.22 at 280 K [Barsi et al., 2003]. The launch of LANDSAT ETM+ was followed by the introduction of the first Earth Observing System (EOS) platform, subsequently named Terra, which included the Advanced Spaceborne Thermal Emission and Reflection Radiometer (ASTER) with five thermal infrared spectral bands, each with a spatial resolution of 90 m and NEΔT of ≤ 0.3 K at 280 K [Yamaguchi et al., 1998]. These new instruments provide an opportunity to develop new applications with thermal infrared data in order to address key scientific questions that could not be addressed with earlier instruments [Steissberg et al., 2005].

This paper is our first step to investigate the potential of medium resolution satellite TIR data in monitoring SST anomalies due to various environmental pollutants at two Apulian coastal sites, Brindisi and Taranto respectively (Fig. 1). Our analysis was implemented on single LANDSAT and multi-date ASTER data in a remote sensing image processing software environment [ENVI, 2008]. Due to the lack of contemporaneous ground surveying, the resulted maps were qualitatively compared with the SST measures published by the Maritime Department of the Italian Agency for the Environmental Protection and Technical Services (APAT).

DATA AND METHODS

Study case 1. The coastal water area of Brindisi

The first analysis was conducted on one LANDSAT ETM+ TIR data set (acquisition date: July 6th, 2001) from the Southern coast of Brindisi which hosts ENEL "Federico II" power plant. The plant complex includes 4 sections divided by polycombustible thermoelectric power of 660 MW each, that came into service between 1991 and 1993. This plant made Brindisi a leader in the production of electricity in Italy. The area considered suffers from severe environmental problems, not only in terms of atmospheric pollution from coal combustion but also of sea bed degradation near the heat water discharges of local cooling ponds [Akella et al., 2009].

To improve the accuracy of thermal pollution identification in TIR sensor data, the high resolution panchromatic data (15 m) was co-georeferenced (reference system UTM 33 – WGS 84) in order to verify the coastal line coincidence in both the images.

LANDSAT ETM+ and ASTER sensors acquire surface temperature data and store it as 8 bit DNs. In order to convert these DNs to temperature data, the procedure was subdivided in two phases, the first for data calibration and the second one for radiometric temperature identification [Zhang et al., 2008].

Radiometric calibration was preliminarily carried out to derive thermal radiance (L_{sensor}). The Digital Number (DN) values of band 6 were converted into spectral radiance L ($W \times m^{-2} \times sr^{-1} \times \mu m^{-1}$) using the following equation:

$$L_{sensor} = gain \cdot DN + offset \qquad [1]$$

This is also expressed as:

$$L_{sensor} = L_{min} + ((L_{max} - L_{min}) / 255) \cdot (DN - L_{min}) \qquad [2]$$

where L_{max} and L_{min} are the spectral radiance values for band 6 at digital numbers 1or 0 and 255, respectively. Moreover, it is known that band 6 of LANDSAT ETM+ is always acquired in low (L) and high (H) gain states. Band 6L provides an expanded dynamic range and lower radiometric sensitivity and can measure temperatures in between –70 ℃ and +90 ℃, whereas band 6H has higher radiometric sensitivity (although it has a more restricted dynamic range) and can measure temperatures in between -30 ℃ and +60 ℃. For band 6L, L_{min} = 0.0, L_{max} = 17.04; for band 6H, L_{min} = 3.2, L_{max} = 12.65.The values for all these parameters were obtained from data header files.

Next, the spectral radiance L_{sensor} was converted into at-sensor brightness temperature T in Kelvin. The conversion formula is given by:

$$T_{sensor} = \frac{K_2}{\ln\left(\frac{K_1}{L_{sensor}} + 1\right)} \qquad [3]$$

where T is the at-sensor brightness temperature in K; K_1 (666.09 K) and K_2 (1282.71 K) are calibration constants.

The resulting SST map was in our case not validated due to the lack of ground based temperature measurements at the time of the satellite overpassing the instruments mounted on the stations located across the study area.

The accuracy and precision of deriving surface temperatures from LANDSAT TM band 6 data have been already assessed in a study by Schneider and Mauser (1996), who employed a full atmospheric model to convert at-satellite radiance to an accurate measure of water leaving radiance (and thus water temperature) at a lake in Germany for which extensive in situ water temperature data were available. On average (across 31 images), atmospheric correction increased satellite derived temperatures by 1.33 K between 9:00 and 11:00 h, the standard crossing times of LANDSAT satellites. Humes et al. (2005) proved that TM-derived temperature was slightly higher than the ground based temperature (approximately 1.5 ºC). With most current satellite observations at 1 km pixel scale, significant variations in near surface meteorological conditions may be observed, depending on surface conditions. Methods using satellite data indicate at least a ≈ 3 K uncertainty in the estimate of SST when compared to standard weather station observations [Goward et al., 1994; Prince et al., 1998]. Thus, we may expect to slightly underestimate temperatures when corrections are not made, although the exact error shall depend upon specific atmospheric conditions.

In our case study, to effectively improve the visual interpretation of SST variations in the processed image, the *Linear with Saturation Stretching* function was lastly applied (Fig. 2). A linear stretch clipped off a portion of the histogram tails and then effectively increased the dynamic range by stretching the remaining histogram over the full 0–255 data range. The pixel values in the lower portion of the histogram were automatically set to 0 and the values in the upper portion of the histogram clipped were set to 255.

Study case 2. The coastal water area of Taranto

The coastal water area in the Gulf of Taranto (Ionian Sea) was investigated in this study because of its complex environmental system. It consists of a coastal marine area between two sea basins known as “Mar Grande” and “Mar Piccolo”. Mar Grande is characterized by the presence of important naval and industrial activities. This sea area is connected to the basin of Mar Piccolo by two narrow channels, the so-called “Navigabile” and “Porta Napoli” channels. Mar Piccolo washes the Northern town area of Taranto. It is an inner, semi-enclosed basin with a 21 km2 surface area, divided into two inlets, called first and second inlet, which have a maximum depth of 13 and 8 m, respectively. Its a marine ecosystem features a number of lagoons, strongly modified by human activities. Being a semi-enclosed basin, it is affected by water exchange mainly due to its moderate tidal range which does not exceed 30-40 cm [De Serio et al., 2007]. The source of pollution in Mar Piccolo mainly originates from urban effluents, discharges from local industries, spillages from vessels, harbour operations, and presumably atmospheric transport [Mossa, 2006]. In addition, a large industrial settlement (the most important steelworks in Europe) and a petroleum refinery also affect the neighborhoods of Taranto, while small rivers and freshwater springs drain the surrounding agricultural soils in the basin of Mar Piccolo [Pisoni et al., 2004; Cardellicchio et al., 2007].

The analysis of this study area was carried out on the multi-date TIR bands of ASTER sensor data (acquisition dates/time: August 11th, 2000 – time 10:07; June 18th, 2006 - time 9:46; August 24th, 2007- time 9:46). As in study case 1 above, temperature data was obtained through two conversion phases.

First, digital number (DN) values of thermal infrared bands were converted into spectral radiance *Ls* ($W \times m^{-2} \times sr^{-1} \times \mu m^{-1}$) using the following equation:

$$L_{sensor} = gain \cdot (DN - 1) \qquad [4]$$

where gain is different in every band:

gain(10) = 0.006882, gain(11) = 0.006780, gain(12) = 0.006590, gain(13) = 0.005693, gain(14) = 0.005225.

Secondly, spectral radiance was converted into brightness temperature by means of the following equation:

$$T_{sensor} = \frac{c_2}{\lambda_c \ln\left(\frac{c_1}{\lambda_c^5 (L_{sens} + 1)}\right)} \qquad [5]$$

where:

$c_1 = 1.191 \times 108\ Wm^{-2}\ sr^{-1}\ \mu m^{-1}$, $c_2 = 1.439 \times 104\ \mu m\ K$, λ_c is the wavelength in μm.

The resulting SST showed substantial concordance with the ground based temperature measurements taken at the time of the satellite overpassing the mareographic station (SM3810 model) located at the pier St. Eligio in Taranto’s harbor. Such measurements were published by the Maritime Department of the

Italian APAT. At 10:00 h, the crossing time of ASTER satellites, the measured temperatures were: August 11th, 2000 – 24.5 °C; June 18th, 2006 - 22.0 °C; August 24th, 2007- 27.2 °C.

Lastly, to make previous image treatments more effective and enhance the interpretation of SST variations in the processed image, the Linear with Saturation Stretching function was implemented in this study case, too.

RESULTS AND CONCLUSIONS

The final data from both study cases were interpreted in order to better understand the environmental processes impacting on both areas.

The SST values derived from LANDSAT thermal data were divided in two distinct zones (zone 1 and zone 2) in the coastal area of Brindisi, with 20.51 °C (T1) and 23.25 °C (T2) values as mean temperatures (Fig. 3). The rate of change in temperature T between zone 1 and zone 2 was then calculated, normalizing the difference between T1 and T2.

$$\Delta T(\%) = (T_1 - T_2)/T_2 \times 100 = 13.26\% \qquad [6]$$

The resulting SST spatial distribution combined with the obtained increase in temperature ΔT between zone 1 and zone 2 demonstrated the effectiveness of this image data analysis in rising up thermal anomalies in sea water.

As to SST spatial and temporal distribution in the Gulf of Taranto's study area, a qualitative analysis of the time series processed ASTER showed a progressive increase of temperature, especially for 2007 data. The resulting image showed a significant SST rise for the second inlet of Mar Piccolo, correlated to its scarce hydrodynamics. As for the first study case, the prevalence of temperature anomalies can't but emphasize the vulnerability of the coastal area studied.

The examination of results as presented in this study shows the effectiveness of satellite methods and technologies in thermal monitoring of coastal areas subjected to intense atrophic activities. The SST maps derived from both TIR LANDSAT and ASTER sensors captured fundamental properties such as minimum and maximum temperatures, dates of temperature extremes, and rates of change in temperature, all useful in understanding estuarine and coastal processes which could hardly be recognized through lower spatial resolution.

In order to provide reliable information on favorable and unfavorable environmental conditions and in the water area studied, permanent monitoring should be maintained on major ground based parameters (current fields, wind speed and direction, air temperature, etc.). Such monitoring should be performed by processing and analyzing remotely sensed data and comparing it with the results of in-situ measurements. When new satellite techniques aimed at generating, organizing, storing, and analyzing spatial information are combined with watershed, estuarine and coastal ecosystem models, coastal managers and scientists have sufficient means to assess the impacts of alternative management practices.

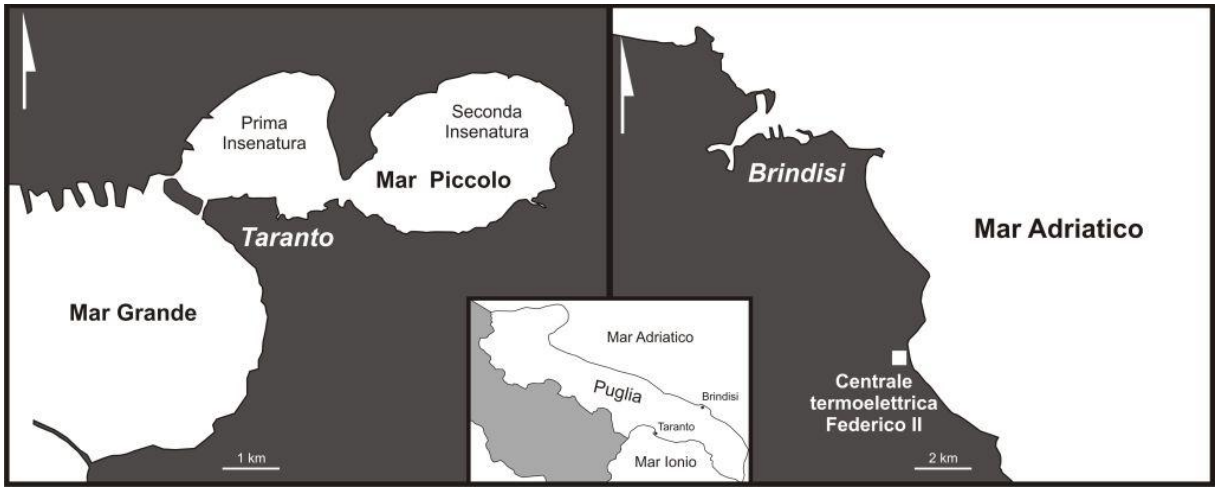

Figure 1 – The two study sites along the Apulian coast.

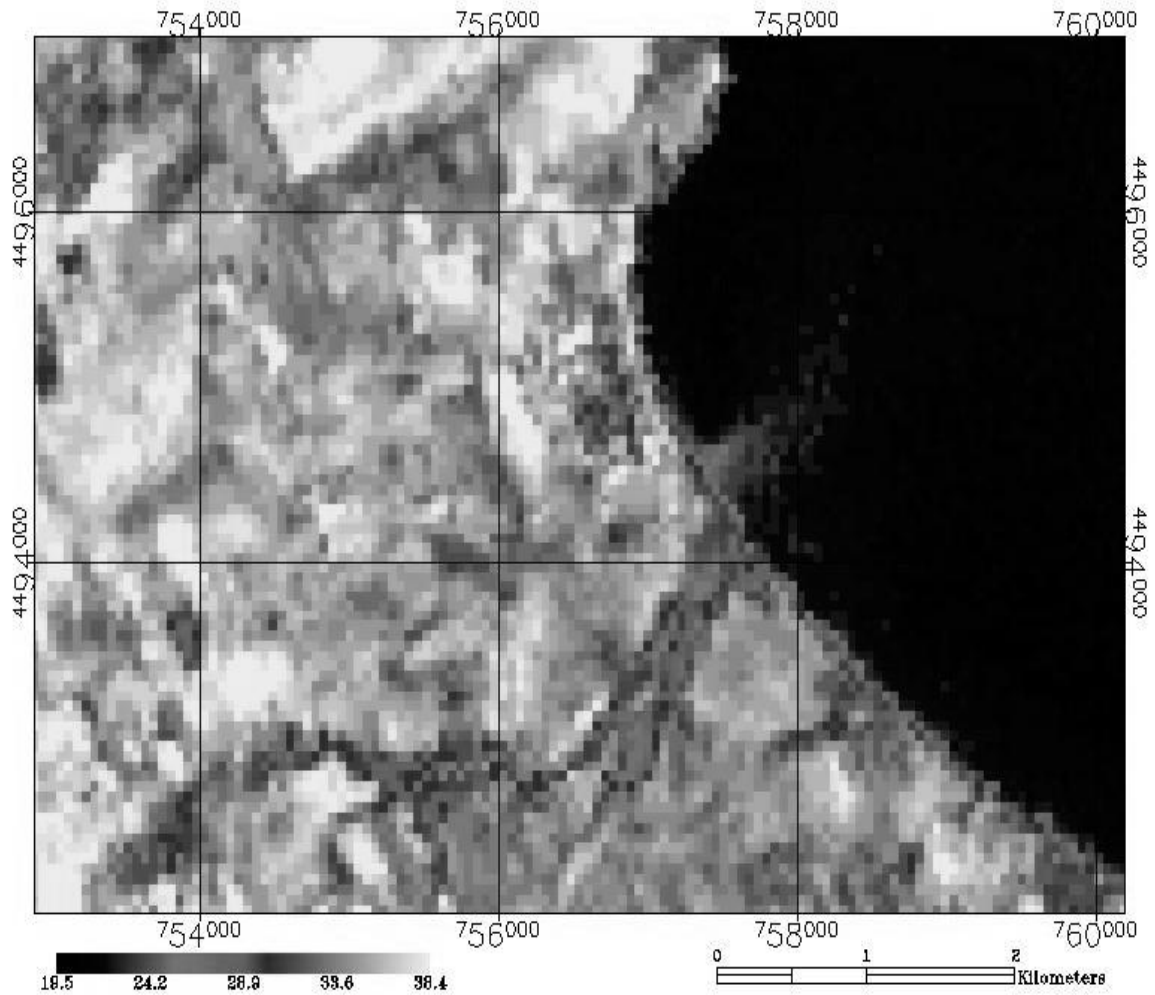

Figure 2 – Map showing the spatial distribution in °C of Sea Surface Temperature (SST) near the power plant "Federico II" of Brindisi (acquisition date: July 6th, 2001).

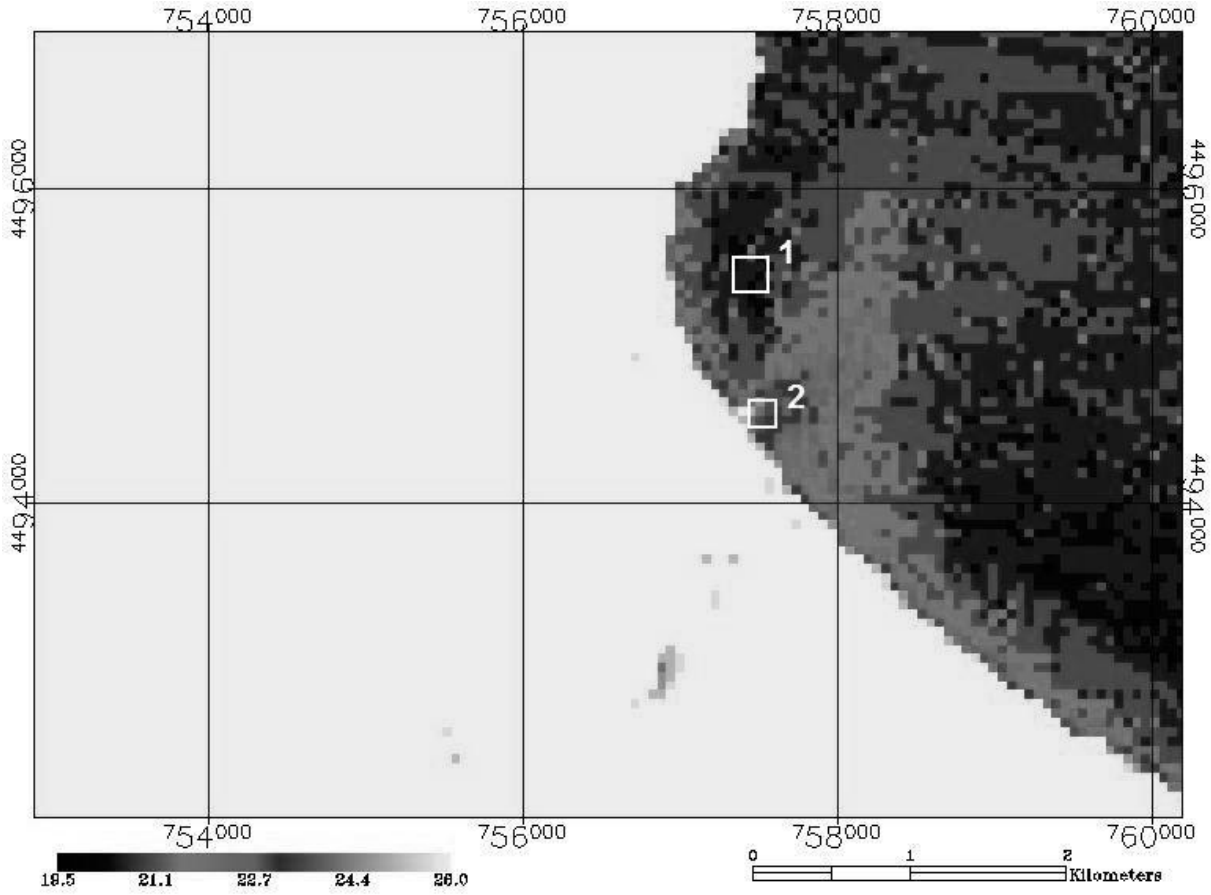

Figure 3 – Identification of zones 1 and 2 for the calculation of SST variation near the power plant "Federico II" – Brindisi.

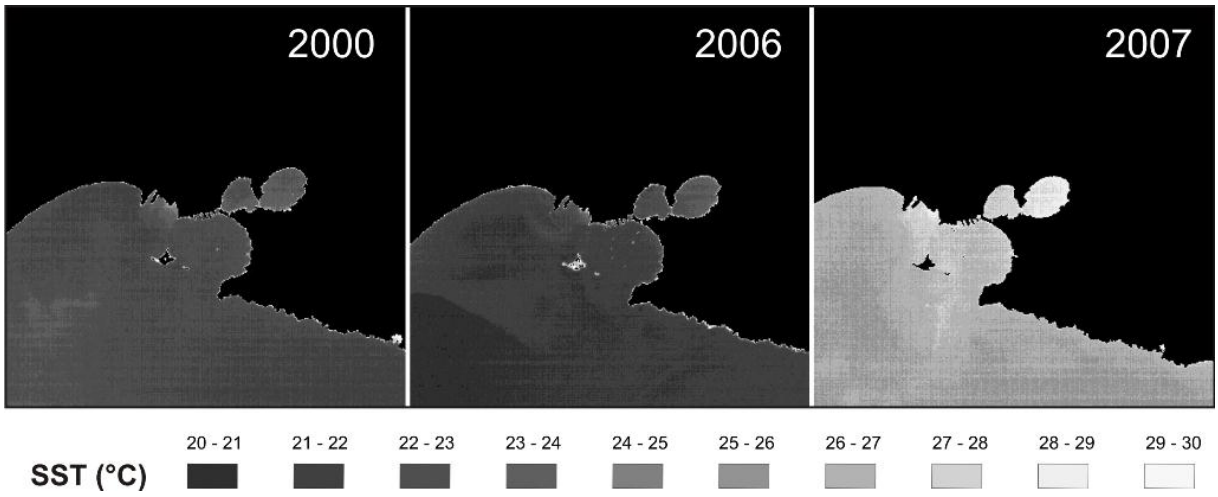

Figure 4 – The SST changes identified on the multi-date TIR ASTER data (2000, 2006 and 2007) in the marine coastal area between Mar Grande and Mar Piccolo – Taranto.

REFERENCES

Akella A. K., Saini R. P., Sharma M. P. (2009) - Social, economical and environmental impacts of renewable energy systems. Renewable Energy, 34: 390–396.

Barsi J. A., Schott J. R., Palluconi F. D., Heider D. L., Hook S. J., Markham B. L., et al. (2003) - LANDSAT TM and ETM+ thermal band calibration. Canadian Journal of Remote Sensing, 29(2): 141–153.

Bondur V. (2005) - Complex Satellite Monitoring of Coastal Water Areas. Proceed. of 31st Int. Symp. on Remote Sensing of Environment. St. Petersburg.

Cardellicchio N., Buccolieri A., Giandomenico S., Lopez L., Pizzulli F., Spada L. (2007) - Organic pollutants (PAHs, PCBs) in sediments from the Mar Piccolo in Taranto (Ionian Sea, Southern Italy). Marine Pollution Bulletin, 55: 451–458.

Choubey V. K. (1998) - Laboratory experiment, field and remotely sensed data analysis for the assessment of suspended solids concentration and Secchi depth of the reservoir surface water. International Journal of Remote Sensing, 19(17): 3349– 3360.

De Serio F., Malcangio D., Mossa M. (2007) - Circulation in a Southern Italy coastal basin: Modelling and field measurements. Continental Shelf Research, 27: 779-797.

ENVI's User Guide. ITT Visual Information Solutions, 2008.

Goward S.N., Waring R. H., Dye D. G., Yang J. (1994) - Ecological remote sensing at OTTER: satellite macroscale observations. Ecological Applications, 4: 322–343.

Humes K., Hardy R., Kustas W. P., Prueger J., Starks P. (2005) - High spatial resolution mapping of surface energy balance components with remotely sensed data. Thermal Remote Sensing in Land Surface Processes. Quattrochi D. A. and Luvall J. F. Editors. Taylor & Francis e-Library, Boca Raton, Florida. pp. 110-132.

IPCC, 2010: Meeting Report of the Intergovernmental Panel on Climate Change Expert Meeting on Assessing and Combining Multi Model Climate Projections [Stocker, T.F., D. Qin, G.-K. Plattner, M. Tignor, and P.M. Midgley (eds.)]. IPCC Working Group I Technical Support Unit, University of Bern, Bern, Switzerland, pp. 117.

Klemas, V. V. - Remote Sensing of Coastal Resources and Environment. Environmental Research, Engineering and Management, 2(48): 11-18.

Ikeda M., Dobson F. W. (1995) - Oceanographic Applications of Remote Sensing. CRC Press, New York.

http://www.idromare.it/ (accessed on December 2nd, 2010).

Mossa M. (2006) - Field measurements and monitoring of wastewater discharge in sea water. Estuarine, Coastal and Shelf Science, 68: 509-514.

Pisoni M., Cogotzi L., Frigeri A., Corsi I., Bonacci S., Iacocca A., et al. (2004) - DNA adducts, benzo(a)pyrene monooxygenase activity, and lysosomal membrane stability in Mytilus galloprovincialis from different areas in Taranto coastal waters (Italy). Environmental Research, 96: 163–175.

Prince S. D., Goetz S. J., Dubayah R. O., Czajkowski K. P., Thawley M. (1998) - Inference of surface and air temperature, atmospheric precipitable water and vapor pressure deficit using Advanced Very high-Resolution Radiometer satellite observations: comparison with field observations. Journal of Hydrology, 212–213: 230–249.

Rogers R. H., Shah N. J., McKeon J. B., Smith, V. E. (1976) - Computer mapping of water-quality in Saginaw Bay with LANDSAT digital data. Photogrammetric Engineering and Remote Sensing, 42(6): 831.

Schladow, S. G., Palmarsson, S. O., Steissberg, T. E., Hook, S. J., & Prata, F. J. (2004) - An extraordinary upwelling event in a deep thermally stratified lake. Geophysical Research Letters, 31: L15504.

Schneider K., Mauser, W. 1996 - Processing and Accuracy of LANDSAT Thematic Mapper Data for Lake Surface Temperature Measurement. International Journal of Remote Sensing 17: 2027–2041.

Steissberg T. E., Hook S. J., Schladow S.G. (2005) - Characterizing partial upwellings and surface circulation at Lake Tahoe, California–Nevada, USA with thermal infrared images. Remote Sensing of Environmental, 99: 2-15.

Zhang G., Liu J., Fei W. (2008) - Detection of Anomaly Temperature Based on ASTER and ETM+ Thermal Infrared Image. International Conference on Computer Science and Software Engineering, Wuhan, China. pp. 241-244.

Yamaguchi Y., Kahle A. B., Kawakami T., Pniel M. (1998) - Overview of Advanced Spaceborne Thermal Emission and Reflection Radiometer (ASTER). IEEE Transactions on Geoscience and Remote Sensing, 36(4): 1062–1071.